AD-A009 101

MICROWAVE WAVEGUIDE MODULATORS FOR CO_2 LASERS

P. K. Cheo, et al

United Aircraft Research Laboratories

Prepared for:

Office of Naval Research
Advanced Research Projects Agency

31 March 1975

R921513-10

Fifth Semi-Annual Technical Report

Microwave Waveguide Modulators For CO_2 Lasers

by

P. K. Cheo, D. Fradin and R. Wagner
United Aircraft Research Laboratories
East Hartford, Connecticut 06108

March 31, 1975

Principal Investigator: P. K. Cheo (203) 565-4297

Prepared for the Office of Naval Research
Contracting Officer: Dr. M. White
Contract No. N00014-73-C-0087
Contractor Modification No. P00003 - $313.780
25 September 1974 to 25 March 1975

Sponsored by
Advanced Research Projects Agency
ARPA Order 1860, Amendment No. 6

TABLE OF CONTENTS

(3) */dodn+11[illegible]:12111.1111

1) AD-787 47[illegible] C 2) 20/5 * 46C
4) PC$3.75/MF$2.25
5) United Aircraft Research Labs., East Hartford, Conn.
6) Microwave Waveguide Modulators for CO2 Lasers.
9) Semi-annual technical rept. no. 4, 25 Mar-25 Sep 74, (10) by P. K. Cheo, M. Gilden, D. Fradin, and R. Wagner. (11) 25 Sep 74, (12) 37p
14) (-AC) UARL-N921513-8, (I--) N921513-8
15) (A) Contract N[illegible]14-73-C-[illegible]87, (A) ARPA Order-186[illegible]
21) *Office of Naval Research, Arlington, Va. *Advanced Research Projects Agency, Arlington, Va.
See also report dated 29 Mar 74, AD-776 663.
evl/GRA 74-26 12 Nov 74

DO NOT PUNCH

Added Entry

74-26

HC

Release Date

Check List for Fields

	DC	SA
1	✓	
2		
4	✓	
5	✓	
6	✓	
8	-	
9	✓	
10	✓	
11	✓	
12	✓	
14	✓	
15	✓	
16		
17		
18		
19		
21		
22		
23		
25		
27		
29	✓	
30		
33	✓	
34	✓	
35	✓	C

23) Descriptors

*Carbon dioxide lasers,
*Laser modulators,
Thin films,
Gallium arsenides,
Infrared lasers,
Gas lasers,
Waveguides,
Phase modulation,
Fabrication,
Nickel alloys,
Copper alloys,
Sidebands,
Ion beams,

25) Identifiers

*Optical waveguides

27) Abstract: See reverse ( ) Page (s) -- 1-1, 1-2

29) Inventory 11

30) Annotated Title

33) Dist. Code 1

34) Serial 4

35) Code 357 370

FORM NTIS-50 (REV. 6-71)

DOCUMENT PROCESSING WORKSHEET

U.S. DEPARTMENT OF COMMERCE
NATIONAL TECHNICAL INFORMATION SERVICE

USCOMM-DC 41420-P71

1.0 TECHNICAL REPORT SUMMARY

1.1 Program Objectives

The long-range objective of this program is to develop an efficient and reliable ultra-wideband waveguide modulator for CO_2 lasers that will be useful for high resolution, imaging optical radars and high-data-rate optical communication systems. Efficiency and reliability are obtainable by using integrated optics technology. Because this technology is still at an early stage of development, many novel concepts must be demonstrated and new techniques developed. Of particular concern during the present program are several critical items which must be investigated in order to maximize the generation of side-band power and to establish the reproducibility of the modulator performance. Specifically, we have experimentally determined the effects of a number of parameters, including the grating configuration, waveguide thickness tolerances, and thin metal layers on the coupling efficiency and propagation losses of both the optical wave and the microwave field. Efforts were also made to improve the waveguide quality and its structural strength by using ion-beam milling and special bonding techniques. This report gives an up-to-date detailed discussion of these effects and presents our technical approach to achieving the long-range objective of this program.

1.2 Major Accomplishments

During this reporting period three significant advances have been made in the modulator development. The first development involves improvements in the quality of the GaAs waveguide structure and the reliability of producing thin-film waveguides with acceptable quality; the second development, which is described in detail in Section 3.0, involves improvements in optical coupling efficiency; and the last development involves improvements in the reproducibility of the microwave characteristics of the waveguide modulator. With the exception of the growth of the bulk GaAs crystals, which are currently purchased from two different vendors, the complete material processing and waveguide synthesis are being carried out at our laboratory under controlled procedures. Waveguide structures with lengths in excess of 2 cm, which include two 3 mm x 3 mm grating couplers at the ends can now be reliably made with any desirable average thickness in the range of 20 to 30μ and with good average thickness uniformity. At present, our production yield is better than 50 percent and the entire fabrication procedure requires approximately three days to complete the entire processing cycle, starting from raw material to optically polished waveguides with grating couplers.

Using grating couplers nearly 7 percent of the incident light has been coupled into a single output beam. This value includes the propagation loss inside the waveguide. Preliminary results indicate that the improvements in mechanical strength permit the use of Ge prism couplers and that at least a factor of two increase in total optical transmission through the waveguide can be achieved by using a prism pair. Both optical and microwave measurements are reproducible to within $\pm$ 5 percent. From optical coupling characteristics, it is possible to determine the quality and physical parameters of the waveguide as discussed in detail in Section 3.0. Optical power densities up to 4 kW/cm^2 have been applied to these waveguides; and at this level, no apparent optical damage has been observed. Excellent reproducibility of microwave characteristic impedance measurements with either ridge or micro-strip configuration has been obtained with the help of copper layers deposited on the surfaces of the waveguide.

1.3 Future Work

A series of experiments will be conducted during the remaining contractual period (March 1975 to June 1975) to perform microwave phase-modulation of a CO_2 laser ($\simeq$ 10 W) at a frequency of about 16 GHz. Waveguide modulators used in these experiments will have an active length of at least 2 cm. Grating and, if appropriate, prism couplers will be employed. With grating coupling, a traveling-wave ridge microwave modulator will be used, whereas a micro-strip microwave structure will be used with the prism coupler. With this latter configuration, a total optical transmission of nearly 15 percent should be possible. Experimental results will be included in the final technical report.

Based on existing data, a reasonable prediction of sideband power can now be made. In the small-phase-shift approximation, the power generated in the sideband is given by

$$P_{SB} \simeq \left(\frac{\Delta\phi}{2}\right)^2 P_T \qquad (1)$$

where P_T is the optical power transmitted through the phase modulator and the phase-shift of the laser beam that results from the interaction with the microwave field is given by

$$\Delta\phi \simeq \frac{\pi n^3 r_{41} L}{d\lambda} \sqrt{Z_o P_\mu} \, . \qquad (2)$$

Here, $n = 3.27$, $r_{41} = 1.2 \times 10^{-10}$ cm/V, L and d are the interaction length and the thickness of the waveguide, $\lambda = 10^{-3}$ cm, and P_μ is the microwave power. The measured impedance Z_o is about 50Ω. For a given input laser power P_o, P_T varies with optical transmission (total optical coupling efficiency) η as

$$P_T = \eta P_o. \tag{3}$$

It is reasonable to assume that P_o = 20 W and P_μ = 100 W can be used with a 20μ thick GaAs slab. In this case, Eq. (1) becomes

$$P_{SB} \simeq 0.107\ \eta\ L^2. \tag{4}$$

The calculated results are plotted in Fig. 1 as a function of waveguide length for three different optical transmission efficiencies: η = 5, 10 and 20 percent. From these curves, it is seen that with a 2 cm long interaction length and a total transmission coefficient of 10 percent, 40 mW of power can be generated in the sideband from a 20 W CO_2 laser. Since the sideband power increases as the square of the interaction length, much can be gained by utilizing longer waveguide structures. Advanced techniques are being developed to produce reliably good quality waveguides having a L greater than 3 cm. With a total coupling efficiency of 20 percent, and a 3 cm long interaction length, we expect to obtain as much as 0.2 W of sideband power from a 20 W CO_2 laser.

FIG. 1

THEORETICAL SIDEBAND POWER

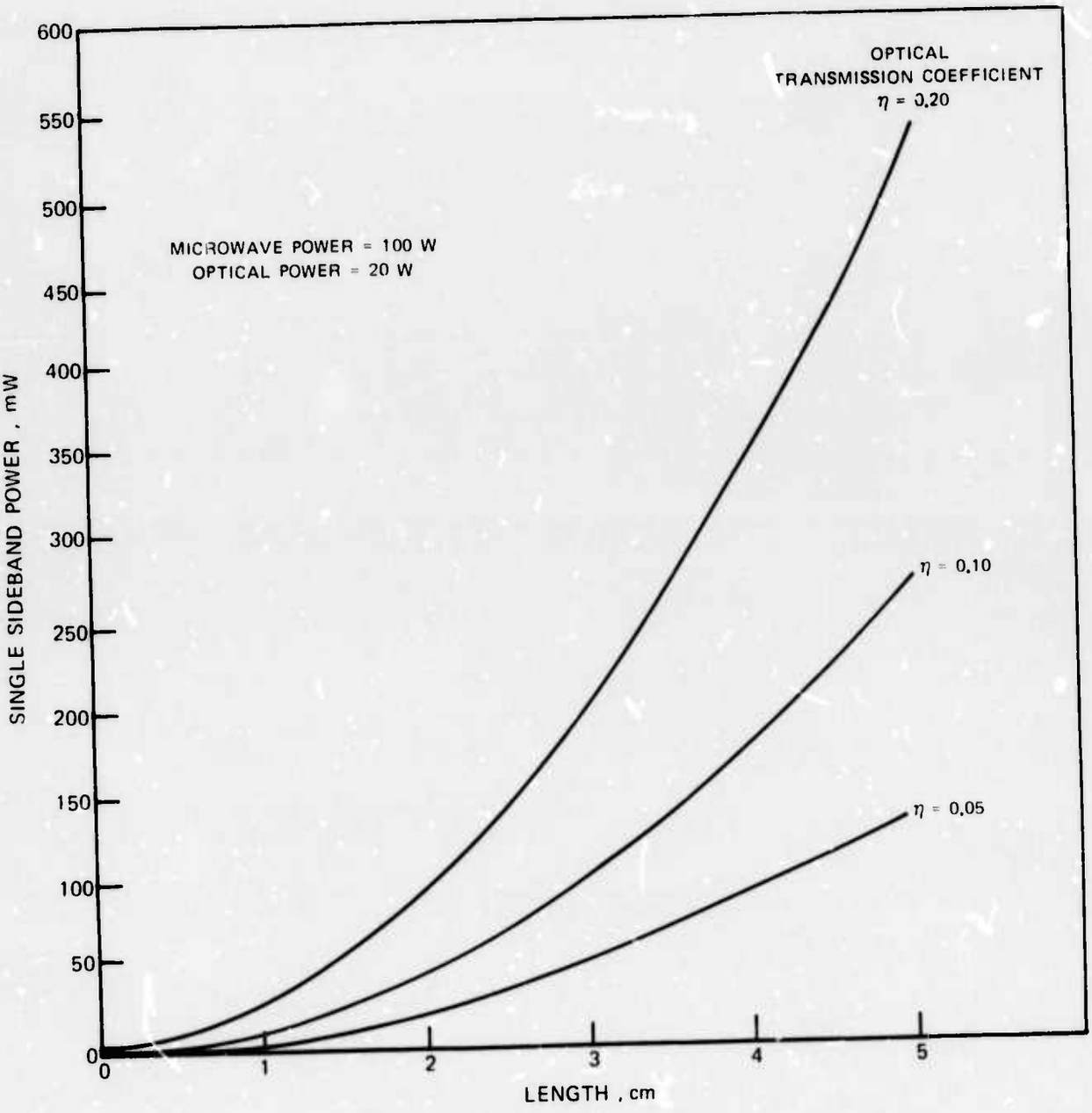

103-188-3

2.0 TECHNOLOGICAL ADVANCES IN WAVEGUIDE STRUCTURES

2.1 Introduction

The first requirement for the thin-film optical device is low optical loss. If the material absorption loss is negligible, the two most significant loss mechanisms are optical coupling and scattering. Optical coupling loss mechanisms will be discussed in greater detail in Section 3.0. This section will address only the scattering loss mechanism and our approach to minimizing this loss. Scattering loss is caused mainly by waveguide imperfections. These imperfections, in our case, are: (1) surface defects, (2) severe thickness variations, and (3) mechanical strains. The seriousness of these imperfections is intimately related to GaAs material thinning and bonding processes. Under the current program considerable effort has been directed to advancing the material processing technology. By utilizing our in-house expertise as well as an outside consultant (Dr. S. Mayberg, Semiconductor Processing Co., Inc., Hingham, MA), we have improved our in-house GaAs material processing capability significantly. The following sections describe in greater detail the various advanced techniques for thinning large-area GaAs wafers. The success of this fabrication effort was primarily responsible, not only for increasing the production yield, but most important, for significantly improving the total optical coupling efficiency through the thin GaAs waveguide structures. In a parallel effort, we are studying the mechanical strain and material defects in thinned G_aAs wafers. Effort in this area is being conducted in collaboration with Dr. H. Posen of Material Division, Air Force Cambridge Research Laboratories.

Also in this chapter we shall discuss techniques currently being developed for ruggedizing the thin GaAs waveguides. In initial experiments ruggedization was achieved by a process that involves first electro-plating an approximately one-mil-thick copper layer onto the GaAs wafers. This wafer is then bonded to an optically flat copper block by a thin ($\sim 1\mu$) layer of indium. The bonded GaAs wafer is then thinned to the desired thickness. Grating couplers, if required, can be fabricated on the surface of the bonded waveguide. In addition to improving the mechanical rigidity of the waveguide, bonding techniques may also be useful for enhancing the thickness uniformity of the waveguide structure.

Figure 2 is a photograph of the ion-beam milling facility. This facility is being used entirely for the fabrication of integrated optical circuits and waveguide devices in support of this research program.

FIG. 2

ION–BEAM MILLING FACILITY

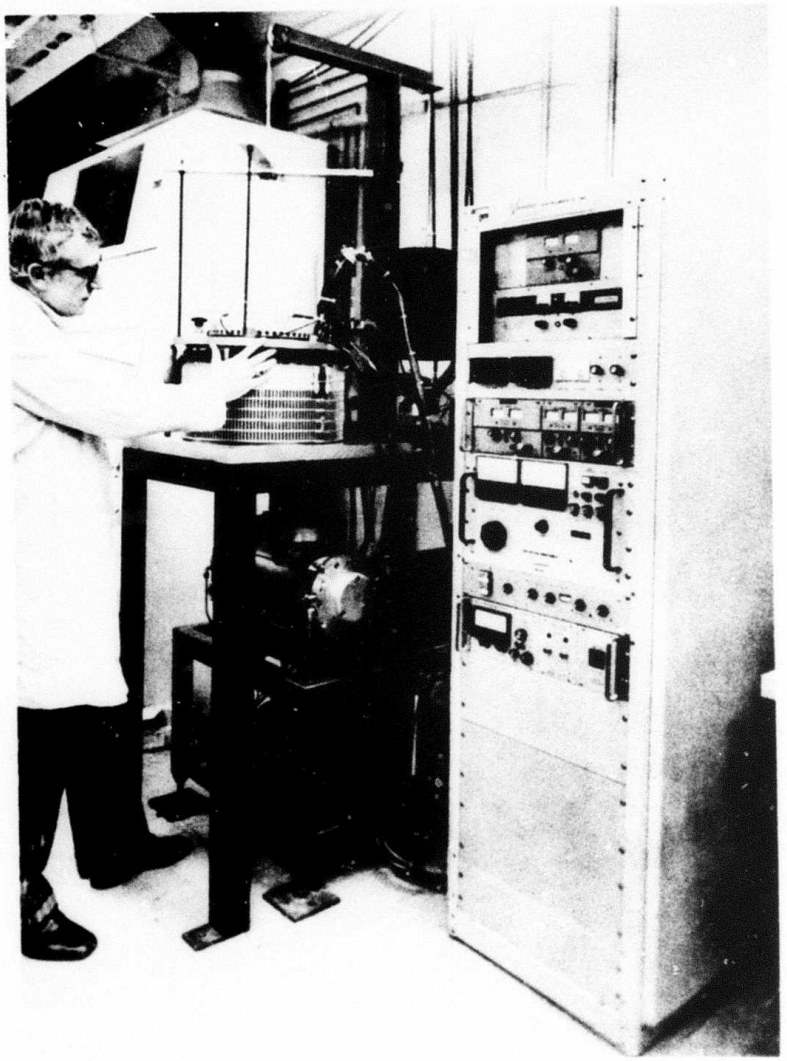

R03-188-2

2.2 Improved Waveguide Fabrication Techniques

A number of waveguide fabrication techniques have been developed during this reporting period. They are intended to improve the optical quality of the GaAs waveguides so that a larger fraction of CO_2 laser power can be transmitted through the single-crystal GaAs thin-film modulator. To accomplish this goal, several requirements with rather stringent tolerance must be met. They are:

1. Gratings must be fabricated with a groove depth, $\delta \gtrsim d/10$, where d is the thickness of the waveguide.

2. The groove aspect ratio a/δ, where a is the ridge of the groove must be controlled.

3. Uniformly thin wafers, with $d \simeq 25\mu$ and $\Delta d < 1\mu$ over a surface area > 1 in^2, must be fabricated.

4. Lapping and polishing techniques that will provide relatively strain-free and microcrack-free thin wafers with improved production yield must be developed.

5. Wafer bonding techniques that will provide the necessary mechanical strength required for practical use must be developed.

2.2.1 Fabrication of Deep Grooves

It is known that the strength of a grating coupler increases with the groove depth, eventually reaching a saturated value as the depth of the groove is increased beyond the penetration depth of the evanescent field of the optical guided-wave. In Section 3 tehoretical and experimental data on optical coupling will be given. Here, new techniques for controlling the grating groove depth are discussed.

Instead of using photoresist for grating fabrication as reported previously (Ref. 1), we have obtained deeper grooves by using a thin titanium mask. This new technique makes use of the fact that the differential milling rate between GaAs and Ti is 10:1, which is about 2.5 times higher than that between GaAs and photoresist film. Two advantages are gained by using Ti films as the mask: (1) deeper grooves, with δ greater than 3μ, have been achieved; and (2) because of high differential milling rate, the Ti mask used for forming phase grating pattern need not be very thick. This latter advantage is important, because it allows the formation of images with much improved edge acuity. The formation of deep grooves utilizes the following procedure:

1. Deposit on GaAs wafer surface a 4000 Å thick positive photoresist film.

2. Expose and develop phase grating image with a iron-oxide mask having the desired periodicity.

3. Ion plate 3000 Å thick Ti film over wafer surface having resisted image.

4. Ion mill grooves into GaAs to desired depth.

5. Lift off titanium-plated photoresist with acetone.

6. Strip remaining titanium in HF.

7. Complete the final thinning of the wafer.

Figure 3a shows a symmetric (saw tooth) grating with a period of 2.75μ that was fabricated in this manner. The groove depth of this grating is also about 2.75μ. With this particular grating profile, the input coupling efficiency (including propagation losses) for the TE_2 mode was as high as 24 percent as indicated by the decrease in the reflected and transmitted powers at the grating coupling angle. The total useful coupling efficiency (including propagation losses) into a single output beam was 7 percent. Because of the quality and good reproducibility of these gratings, the useful coupling efficiencies have increased considerably from our earlier measurements (Ref. 1) and the coupling measurements have been very reproducible. As noted in Section 3, one of the disadvantages of using grating couplers is the generation of one extra beam at each coupler. In general, one half of the optical power will be lost at each coupler if a symmetric grating coupler is used. To alleviate this problem, it has been suggested (Ref. 2) that more optical power can be directed into the useful beam from the undesirable beam by a proper blazing of the grating grooves. For this reason experiments were conducted to produce blazed gratings by varying the incident angle of ion-beam with respect to the mask normal. We found that it is possible to control the blazing angle of grating groove to a reasonable degree of accuracy. A blazed grating fabricated by ion-beam milling at a 45 deg angle of incidence is shown in Fig. 3b.

2.2.2 Improvement of Waveguide Thickness Uniformity

Considerable effort has been directed to improving the thickness uniformity of the thin GaAs wafers. In principle, it is possible to maintain a true parallelism by an extremely careful lapping procedure. However, it is commonly observed that the lapping process produces surface damage in the forms of microcracks that can be substantially reduced by using chemo-mechanical thinning

FIG. 3

ION–BEAM MILLED GRATING COUPLERS WITH VARIOUS GROOVE PROFILES

Λ = 2.75 μm

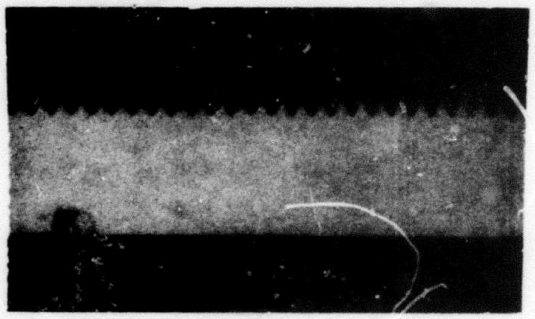

SAW TOOTH ×1000

(a)

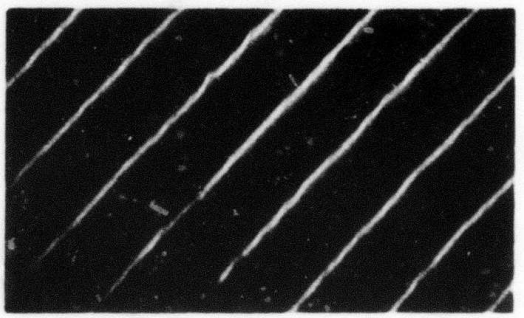

BLAZED ×5000

(b)

R03-188-1

process (Ref. 1). However, this thinning technique introduces wedging or thickness nonuniformities in the wafer as a result of differential etching rates for different crystal planes. Thickness variations are also introduced by nonuniformities in the mounting wax. By using chemo-mechanical polishing, we have observed thickness variations of from 3μ to 15μ over a 2 cm length wafer having an average thickness of 30μ. Severe wedging can reduce the optical coupling efficiency and cause mode conversion.

To overcome this difficulty, a compromised procedure has been developed which involves a combination of lapping, chemo-mechanical thinning, and ion-beam polishing. The procedure starts by taking a saw-cut GaAs wafer having an initial thickness of 15 mils and lapping it carefully down from both surfaces to about 4 mils, while maintaining near perfect surface parallelism. At this point, one mil of material is further removed from each surface by a chemo-mechanical thinning process. The removal of only one mil from a flat surface does not introduce any significant wedging problem, but it can eliminate virtually all mechanical damage and micro-cracks generated by the lapping process. The wafer is now approximately 2 mils thick. To reach the desired waveguide thickness (20 to 30μ), material is further removed from both surfaces by ion-beam milling.

With this procedure, initial experiments using relatively crude polishing equipment produced encouraging results. By updating the polishing apparatus with an instrument manufactured by Geoscience Corp., we were able to consistently produce thin GaAs wafer of 25μ thickness, having an average thickness variation of not more than about 2μ across 3 cm length as determined by an IR spectrophotometer. Local thickness variations (or "wrinkles") were not monitored although the optical coupling experiments in Section 3.0 suggest that they may exist and are a factor in the coupling process. This average thickness variation represents the best tolerance achievable with our current polishing jig. A refined polishing jig, manufactured by Logitech, Ltd. (Scotland), has been ordered and will be used in the near future. This instrument provides much finer angular adjustment than our current polishing jig. With this instrument it will be possible to reduce average wafer thickness variations to less than 1μ over a wafer length of 5 cm.

2.2.3 Structural Ruggedization

Improved lapping and thinning techniques have increased the waveguide production yield to better than 50 percent. Most of the sample failure occurs in the final thinning cycle where the wafer becomes extremely fragile. Furthermore, it is very difficult to handle these thin wafers after the final thinning procedure is completed. To alleviate this problem, techniques are now being developed to bond a semi-thinned GaAs wafer to a thick copper block before completing the waveguide fabrication process. The copper block will be the baseplate in the microwave modulator. Several bonding methods have been considered during this reporting period. They include:

1. Metallization of wafer and bonding to a metal block with solder

2. Eutectic bonding of metallized wafer.

3. Bonding with low viscosity polymer.

4. Reflow bonding with low-temperature glass.

It is premature at the time of writing to discuss relative merits of these methods. We have, however, achieved encouraging results with the first method and have made several waveguide modulators using it. A typical sample is shown in Fig. 4. This device was made by bonding a section of a one-side-polished GaAs wafer (0.160 in. wide by 1.3 in. long by 0.015 in. thick) to an optical polished copper block using 50/50 indium/tin solder. The wafer was metallized on its polished face with 1 mil of copper prior to bonding. After bonding, the wafer was further lapped and chemo-mechanically polished to a thickness of 30μ. Infrared spectrophotometer measurements indicated that this wafer had an average thickness variation of only 1μ across a 3 cm length. As before, localized thickness variations were not monitored.

Method 2, eutectic bonding, is a relatively simple technique that is well-known in the semi-conductor industry. Bonding of long narrow waveguide strips (1.3 in. x 0.160 in.) utilizing this method may require special jigging.

A low viscosity polymer, such as an RTV rubber or a cyanoacrylate ester, should also be suitable for forming a permanent thin-film bond. A possible limiation of this bonding procedure may be the poor thermal conductivity of the bond which can limit the capability for high-power device applications.

Reflow bonding using a low-temperature glass has also been considered. This technique can be particularly useful for bonding prisms to waveguide structures. A low melting chalcogenide glass that transmits at infrared wavelengths beyond 10μ can be made (Ref. 3) of a suitable mixture of As, S, and Se. This glass has a melting point of $\sim 125^{\circ}C$. Controlled thicknesses of this glass can be vacuum coated (Ref. 4) onto either the base of a prism, a waveguide structure, or both. The prism then can be placed on top of the waveguide structure and heated until the glass forms a bond.

2.3 Summary

We have routinely fabricated high-quality GaAs waveguides in a free-standing configuration and have achieved good initial results with a copper bonding technique. The average thickness variation along the length of the waveguide has been reduced in the best case to $< 1\mu$ for a 3 cm waveguide having

GaAs WAVEGUIDE MODULATOR WITH A MICROSTRIP ELECTRODE

1 INCH

FIG. 4

an average thickness of 20μ. Techniques have been developed that produce both symmetric and asymmetric grating profiles with the groove depths greater than 3μ. Efforts are being made to further improve our fabrication techniques of GaAs waveguides with a near-term goal of achieving a total optical transmission through the waveguide of more than 10 percent and an electro-optic interaction length greater than 3 cm.

3.0 OPTICAL EVALUATION OF WAVEGUIDE STRUCTURES

3.1 Introduction

The efficient operation of the thin-film modulator requires that a substantial fraction of the input laser power be coupled through the waveguide and into a useful output beam. Prior to the present reporting period, the total effective optical coupling efficiencies achieved with two grating couplers (input and output) were typically about 1 percent or less, whereas the maximum theoretical coupling efficiency for a symmetric waveguide is 20 percent. In order to increase the waveguide coupling efficiency, three general technical directions are being pursued. First, the baseline waveguide is being carefully studied and improved. This baseline waveguide is a symmetric wafer, and coupling is achieved with two phase grating couplers having saw-tooth groove shapes. Second, optical coupling with Ge prisms is being investigated. With early waveguides, the use of prisms was not practical because of sample breakage. Recent improvements in waveguide fabrication, however, have improved both the optical and structural qualities of the GaAs wafers sufficiently to permit the use of prism couplers in laboratory tests. Finally, various asymmetric waveguide structures and grating geometries are being considered. Such structures include metal-backed waveguides, GaAs wafers with a thin-film of ZnSe or other suitable dielectric, and blazed grating grooves.

In this section the results of extensive studies of the improved baseline waveguide and preliminary measurements obtained with both a prism input coupler and a metal-coated asymmetric waveguide are summarized. Total effective coupling efficiencies of up to about 7 percent (including waveguide propagation losses) have been obtained with the baseline waveguide. Also included in this section are measurements of the susceptibility of two waveguide structures to optical damage. It was found that uncoated GaAs wafers and GaAs wafers coated with a thin Au layer can withstand laser intensities of greater than 4 kW/cm^2 without experiencing optical damage.

Both total effective coupling efficiency and the output beam quality achievable with either grating couplers or prism couplers are sensitive to a number of factors including the imperfections of the optical waveguide in the coupling region. Thickness variations or strains in the coupler region change the value of β/k locally and distort the characteristic aperture field of the coupler. Because of the importance of waveguide thickness variations to optical coupling, a discussion of their effects is given first. Other factors that affect the fraction of input light coupled into a useful output beam are also discussed.

3.2 Effects of Waveguide Imperfections on Input Coupling Efficiency

The total optical coupling efficiency for a coupler pair is equal to the product of the input and output coupling efficiencies. Although waveguide imperfections affect both coupling efficiencies, they have a much stronger effect at the input. For this reason the loss in total coupling efficiency resulting from waveguide imperfections in the two coupling regions can be largely understood by considering only the input coupler.

The reason that output coupling efficiency is little affected by imperfections is that an output coupler can always be made to couple out most of the guided optical energy underneath the coupler by just making the coupler long enough. Imperfections and variations in the output coupling region may cause the coupling to diminish locally and distort the outcoupled beam. In the extreme case, imperfections will scatter a substantial amount of the guided light into air modes at arbitrary angles with respect to the waveguide normal. Nonetheless, even a highly imperfect coupler will remove all the optical energy underneath the coupler if the coupler is sufficiently long.

At the input, on the other hand, the fraction of incident energy that is coupled into the waveguide is sensitive to the precise spatial match between the incident field and the characteristic aperture function of the coupler. As discussed in Ref. 5, p. 15, the input coupling efficiency η can be expressed as a normalized overlap integral in the general form

$$\eta = \frac{1}{2} \frac{\left[\int_0^\infty E_{in}(x,y)\, E_a^*(x,y)\, dx\, dy \right]^2}{\int_0^\infty E_{in}\, E_{in}^*\, dx\, dy \int_0^\infty E_a\, E_a^*\, dx\, dy} \qquad (5)$$

where η has been generalized to two dimensions and the factor of $\frac{1}{2}$ has been included to approximately account for power unavoidably lost to the transmitted beam* (see Fig. 5). Here $E_{in}(x,y)$ is the input laser field, $E_a(x,y)$ is the characteristic aperture field; x is the coordinate along the propagation direction of the guided wave; and y is the coordinate in the plane of the waveguide that is perpendicular to the x-direction. The aperture field $E_a(x,y)$ represents physically the normalized electric field that is coupled out of the waveguide when the coupler is used as an output coupler. If the intensity and phase variations of the input beam E_{in} do not exactly match E_a, then η will be less than 100 percent and incident light will be reflected. In fact, as shown below, if significant phase mismatch exists, the input coupling efficiency will be severely degraded.

---

* A transmitted beam represents a power loss for a symmetric waveguide with symmetric grooves. This power loss, which is discussed in the March 1974 report, can, in principle, be greatly reduced by using either blazed grooves or an asymmetric waveguide structure. The power loss actually varies for different gratings so that the factor of $\frac{1}{2}$ in Eq. (5) should be considered to be only a typical correction.

FIG. 5

GRATING COUPLERS

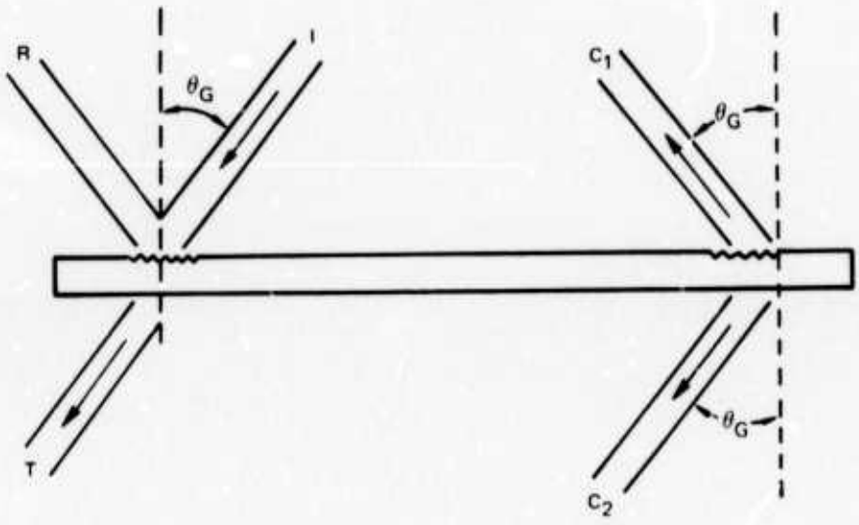

R03-144-1

For a perfect grating coupler, E_a is a function only of x and has the amplitude exp $(-\alpha x)$ where α is the leaky wave parameter or attenuation constant. The phase of E_a is linear in x, thus defining an input coupling angle. If the incident beam has planar phase fronts and is aligned perfectly along the coupling angle, the phase variation of E_a is exactly cancelled in Eq. (5). Assuming that the incident beam is square and uniform in intensity with a beam width in the x-direction equal to ℓ, then Eq. (5) becomes

$$\eta = \tfrac{1}{2} F = \frac{1}{\alpha \ell} [1 - \exp(-\alpha \ell)]^2 \tag{6}$$

as noted in Ref. 5.

In practice, the coupling regions of our present waveguides are not perfectly formed. There are both strains and finite thickness variations in the wafer underneath the guide. Thickness variations are particularly serious because they create large changes in the wave vector β of the guided modes. Strains will also cause β to change but that effect is expected to be small. The grating coupling angle θ_G depends on β through the grating equation

$$\sin \theta_G = \lambda/\Lambda - \beta/k \tag{7}$$

where λ is the incident wavelength, Λ is the groove periodicity, and $k = 2\pi/\lambda$. Consequently, spatial variations in the waveguide thickness in the coupling region create spatial variations in the output coupling angle of the characteristic field E_a. In effect, different portions of the beam couple out at different angles. Under these conditions, it is not possible to completely cancel the phase variations of E_a with a collimated input field E_{in}. A phase dependence persists in the overlap integral of Eq. (5) and η will consequently be reduced.

As an example, let us consider the effects of a slight error in the coupling angle. The input field E_a, which is incident at an angle θ_o with respect to the waveguide normal, contains the linear phase $(k \sin \theta_o x)$. The aperture field contains the phase $(k \sin \theta_G x)$ where $\theta_G = \theta_o + \Delta\theta$ and $\Delta\theta$ is the angular error. Neglecting the y variation of the fields, the overlap integral in Eq. (5) assumes the form

$$\begin{aligned} \int_o^\infty E_{in} E_a^* \, dx &\propto \int_o^\ell e^{i k \sin \theta_o x} e^{-(\alpha + i k \sin \theta) x} \, dx \\ &\cong \int_o^\ell e^{-(\alpha + i k \cos \theta_o \Delta\theta) x} \, dx. \end{aligned} \tag{8}$$

As before, the input field is assumed to be uniform and square with a beam width ℓ. The angular error $\Delta\theta$ has been assumed small. Equation (8) is easily evaluated with the result that η in Eq. (5) is given by

$$\eta = \frac{\alpha}{\ell} \frac{1}{\alpha^2 + a^2} (1 + e^{-2\alpha\ell} - 2\, e^{-\alpha\ell} \cos a\, \ell) \tag{9a}$$

where $a = k \cos \theta_o \Delta\theta$.

Equation (9a) is an oscillatory function with an amplitude that falls rapidly with increasing $\Delta\theta$. If the laser beam is properly aperture matched so that $\alpha\ell = 1.25$, the beam width ℓ is taken as 1 mm, and θ_o is taken as 38 deg (approximate coupling angle for TE_1), than Eq. (9a) can be written as

$$\eta = \frac{1}{2.310 + 98.58(\Delta\theta)^2} [1 - 0.5295 \cos (467.1\, \Delta\theta)] \tag{9b}$$

where $\Delta\theta$ is expressed in degrees. When $\Delta\theta = 0$ deg, η has its maximum value of 40.7 percent. When $\Delta\theta = 1$ deg, however, η is reduced to 1.15 percent. The input coupling efficiency is reduced to half its maximum value when $\Delta\theta \cong 0.153$ deg.

This calculation demonstrates that nearly perfect angular alignment is necessary for efficient coupling. If the coupling region is not uniform, perfect angular alignment will not be possible across the full beam. This fact can be illustrated by considering the effects of a linear thickness variation of the wafer in the coupling region. If this linear thickness variation is small ($\sim 1\mu$), then the grating coupling angle will vary in a nearly linear manner as illustrated by the calculated results in Fig. 6. The linear taper is taken to be along the x-direction so that the coupling angle θ_G is $\theta_o + bx$.

A linear taper is seen to create a quadratic phase variation. The overlap integral in Eq. (5) has the general form [cf. Eq. (8)].

$$\int_o^\infty E_{in}\, E_a^*\, dx \propto \int_o^\ell e^{-\alpha x + i \gamma x^2}\, dx. \tag{10}$$

Inserting this result into Eq. (5) gives

$$\eta = \frac{\alpha}{\ell} \left[\left(\int_o^\ell e^{-\alpha x} \cos \gamma x^2\, dx \right)^2 + \left(\int_o^\ell e^{-\alpha x} \sin \gamma x^2\, dx \right)^2 \right]. \tag{11}$$

GRATING COUPLING ANGLES AS A FUNCTION OF WAVEGUIDE THICKNESS

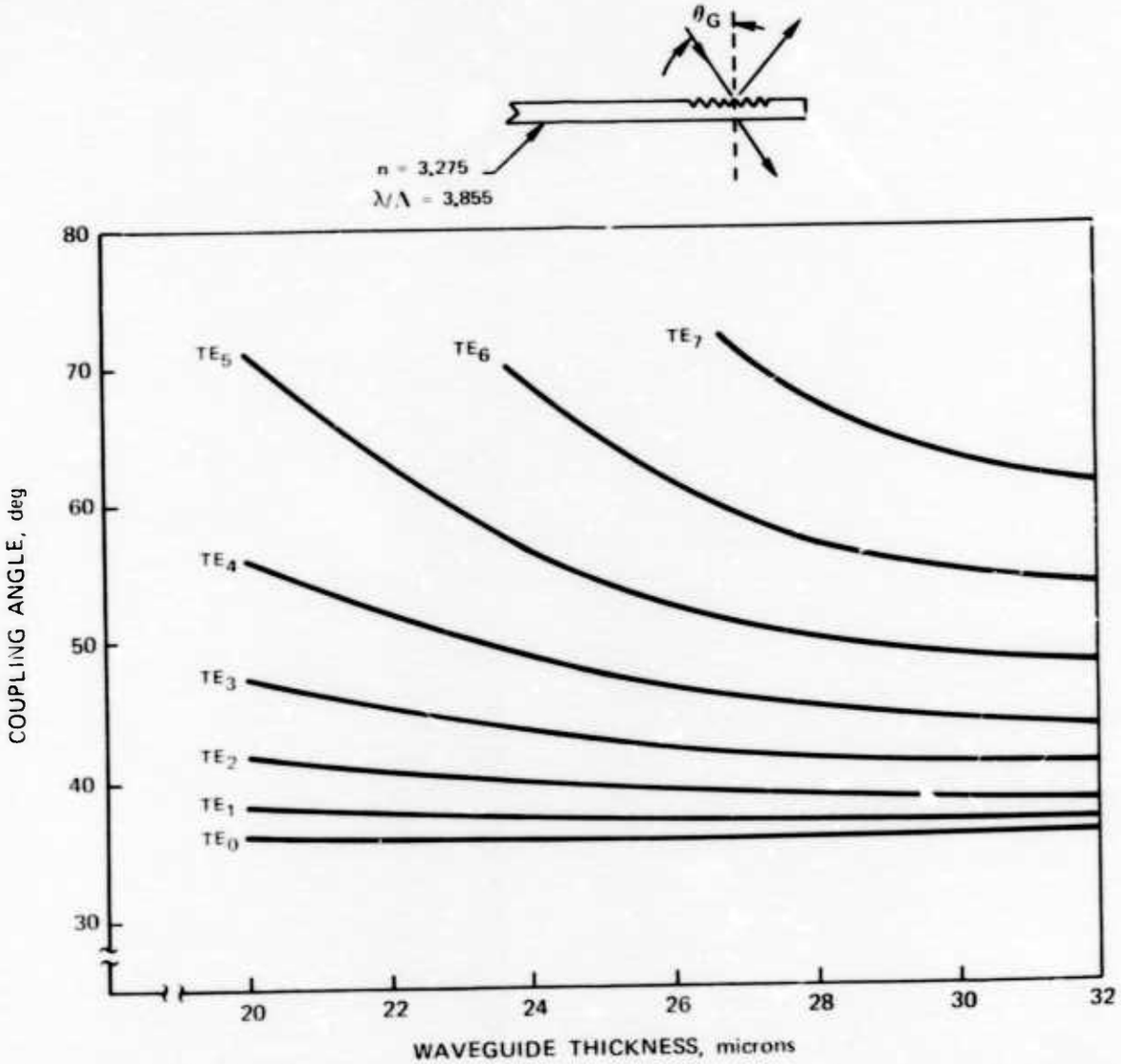

FIG. 6

The integrals in Eq. (11) can be expressed in terms of the well-known Fresnel integrals when $\alpha\ell \ll 1$. For conditions of interest, the incident light beam will be aperture-matched so that $\alpha\ell = 1.25$ and, unfortunately, the Fresnel integral tables cannot be used. Since the integrals in Eq. (11) cannot be expressed in analytical form, a numerical calculation of Eq. (11) is required. At the present time, such a calculation has not been conducted.

Despite the fact that a closed-form solution of Eq. (11) is not possible, a reasonable approximation to η can be made by considering the simpler results of Eq. (9). As noted above, Eq. (9) indicates that an angular error of only 0.153 deg for the TE_1 mode reduces the coupling efficiency to half its peak value. Nearly the same value applies to the other waveguide modes under conditions of aperture matching. The effects of a linear taper may thus be estimated by assuming that coupling effectively occurs only over that portion of the grating for which the angular error introduced by the taper is < 0.153 deg.

Let the waveguide taper be such that over a distance ℓ = 1 mm the coupling angle has changed by 0.5 deg from θ_o to θ_o + 0.5 deg. As discussed below, a taper on the order of 1μ is sufficient to produce this change. The angular error thus reaches 0.153 deg at x = 0.153/0.5 = 0.306 mm where x = 0 is the coupler edge. If aperture matching would be achieved in the absence of the taper, then $\alpha\ell$ = 1.25. Using Eq. (9) with ℓ = 1 mm, the input coupling efficiency is found to be

$$\eta = \frac{1}{\alpha\ell}\left(1 - e^{-0.306\ \alpha\ell}\right)^2 = 0.081 = 8.1 \text{ percent} \qquad (12)$$

as compared to about 40 percent in the absence of a taper.

As apparent from the calculation in Fig. 6, which relates coupling angle to waveguide thickness, the thickness taper needed to produce a coupling angle variation of 0.5 deg is large for the lowest order modes, but the effect of the taper increases rapidly with increasing mode number. For example, if the average waveguide thickness in the coupling region is 25μ, then a negative taper of about 8μ across the 1 mm input beam is necessary to produce a 0.5 deg variation for the TE_0 mode. A taper of this size is large and easily observed. However, a thickness variation of only about 1.3μ for TE_2 and about 0.6μ for TE_3 produces the same effect. A thickness variation of 0.7μ across the input beam is large enough to cause a maximum angular error of 0.27 deg for TE_2 and a consequent drop in the input coupling efficiency from about 40 percent to 20 percent for that mode. Thickness variations of order 1μ are small and are difficult to completely eliminate for the free-standing GaAs waveguides used in the baseline modulator.

These calculations are intended to demonstrate that thickness variations of the order of 0.5 to 1μ in the waveguide coupling region can have a strong effect on the input coupling efficiency. Although the present calculation has considered only a taper along the propagation direction, it should be clear that a transverse taper will degrade the coupling efficiency by nearly the same amount. Thickness variations of this magnitude may occur because of "wrinkles" introduced by the mounting wax in the initial wafer thinning and processing. Alternately, they may occur during the grating fabrication. Since grooves are etched into the waveguide, the effective wafer thickness in the coupling region is reduced by approximately half the groove depth, where the groove depth is typically 1.5 to 2.5μ. Any variations in groove depth across the grating will thus lead to a variation in the effective waveguide thickness in the coupling region. Both wafer thickness variations and significant groove depth variations are observed in the GaAs waveguide structures. Because these variations can significantly degrade the coupling efficiency, considerable effort has been directed at minimizing them. Most of the improvements in useful coupling efficiency achieved during the present reporting period are, in fact, the results of those improvements in the fabrication procedures that have led to more uniform waveguide structures. The considerations discussed here thus provide direction for the waveguide fabrication, as well as clarifying various experimental observations made during the waveguide optical evaluation studies.

In addition to thickness variations, severe strains or any effect that locally changes the index of refraction in the coupling region will reduce the coupling efficiency. Phase distortions in the incident laser beam or strong variations of α along the plane of the coupler resulting from variations in groove geometry will also reduce η. For some waveguide structures these effects may, in fact, be more deleterious than thickness variations. Because of the nature of the thin-film modulator waveguide, imperfections in the coupling region appear to be a significant factor in determining the optical coupling efficiency.

Although the grating coupler has been emphasized in this discussion, the results derived here apply directly to the prism coupler. As discussed in Ref. 5, the prism input coupling efficiency is also given by Eq. (5) with the minor modification that the factor of $\frac{1}{2}$ is absent for the prism case since the prism coupler is, in effect, a single-port directional coupler.

The above discussion has considered only the input coupling efficiency η. The fraction of incident light actually coupled out from the waveguide structure is always less than η. Two additional factors further reduce the amount of useful output power. The first factor is, of course, the optical losses introduced by the output coupler, and the second factor is waveguide propagation losses from attenuation and scattering.

Output coupling losses may result from the existence of an extra diffracted beam or from the fact that for low-order modes the output coupler may not have sufficient length to couple all the guided optical energy. The extra diffracted output beam, which is illustrated in Fig. 5, is always present for a symmetric waveguide having a grating output coupler with symmetric grooves. In general, the extra beam carries half the available output energy so that the available total coupling efficiency is further reduced by a factor of 2. This loss is not present with the prism coupler. The loss associated with uncoupled guided light can be eliminated by increasing the coupler length or the coupling strength. For a grating coupler the coupling strength is increased by increasing the groove depth and, for a prism coupler, by decreasing the air gap separating the prism from the waveguide.

Waveguide propagation losses are potentially serious for coupler separations $\gtrsim 2$ cm. At the present time such losses have not been accurately determined, although it appears that they are not more than about 50 percent for a 2 cm coupler separation. Some propagation losses undoubtedly occur in the two coupling regions so that the observed propagation coefficient will increase with coupler separation L as $C_1L + C_2$ where C_1 and C_2 are positive constants. The total attenuation from such losses will thus scale as $\exp\left[-(C_1L + C_2)\right]$ where C_1 is estimated to be of order 0.25 cm^{-1} or less.

In summary, it has been shown that thickness variation can significantly degrade the achievable coupling efficiency. Other factors such as output coupling losses and propagation losses will further degrade the fraction of incident light that can be obtained as useful output. Table 3.1 summarizes order-of-magnitude estimates of typical optical losses that result from these various loss processes for the present baseline waveguide structure. Despite the significant magnitudes of these various losses, it is shown in Section 3.4 that total effective coupling efficiencies that are within a factor of about 3 of theoretical maximum have been obtained with the baseline waveguide structure.

3.3 Experimental Procedures

The ongoing optical measurements with the baseline waveguide structure are intended both to evaluate the grating couplers in terms of total effective coupling efficiency (including waveguide losses) for the lowest order modes and to establish the dependence of grating performance parameters on various physical parameters including groove geometry, waveguide thickness uniformity, and input laser beam width. Particular goals are to establish standardized test procedures for waveguide evaluation and study, to accumulate a sufficient data-bank on grating performance so that modifications in the fabrication procedures can be suggested and appraised, to increase the coupling efficiency into a low-order mode by a significant amount for a 1-mm beam size, to experimentally determine the importance of various optical loss mechanisms, and to

TABLE 3.1

ESTIMATES OF TYPICAL COUPLING

LOSS EFFECTS - BASELINE WAVEGUIDE

Typical Useful Coupling Efficiency $\cong$ 5 percent

EFFECT	LOSS - dB
Coupler Imperfections	4.0
Propagation Losses (2 cm path)	2.0
Mode Conversion	< 0.1
Scattering at Input	< 0.2
TOTAL	6.0 to 6.3

investigate the performance of alternative waveguide and coupler configurations. In addition, measurements are being conducted to establish the susceptibility of waveguide structures to optical damage. Such measurements are needed to demonstrate that waveguide performance can be scaled to higher incident laser powers.

The experimental arrangement for the optical evaluation of waveguides is illustrated in Fig. 7. A sealed-tube, low-pressure CO_2 laser with a discharge length of 30 cm is used as the optical source. Line selection is achieved by length tuning the cavity with a PZT stack on which the back reflector is mounted. Because the laser resonator is nearly confocal, the transverse modes are spaced in frequency by about $c/4L$ and length tuning with the PZT stack also provides transverse mode selection. With occasional adjustments of the PZT drive voltage, the laser output can be maintained in a TEM_{00} mode at a power level of about 3 W. The beam, which is collimated by a mirror of properly selected radius of curvature, has a diameter ($1/e^2$ in intensity) of about 3.5 mm at the adjustable aperture. A CO_2 laser spectrometer is used for continuous monitoring of the laser power, and the oscillation transition and a rotating aperture wheel chops the beam in order to facilitate accurate measurements with a cooled photodetector and oscilloscope.

The waveguide structure is positioned on an optical mount that can be rotated and moved linearly in three directions. As adjustable aperture is used to control the input beam diameter so that the input beam can be aperture matched (i.e., so that $\alpha\ell \approx 1.25$ as discussed in Section 3.2). At the input grating the apertured beam is collimated with a nearly uniform intensity distribution. Although aperturing the beam significantly reduces the incident laser power, aperturing is a convenient means for adjusting the incident beam diameter without changing the optical alignment. Optical measurements are also obtained with the full laser beam focused to a small spot diameter.

As illustrated in Fig. 7, the optical energy incident on the baseline waveguide structure is distributed among four optical beams (viz, reflected and transmitted beams and two output beams, C_1 and C_2) with some optical energy lost to scattering and absorption in the waveguide structure. For the lowest order mode, TE_0, the grating is not sufficiently long to couple all of the guided mode energy into a diffracted free space beam. Some of the guided energy thus leaks out the output end of the waveguide and can be detected. It has also been found that a small fraction of the guided optical energy leaks out the end on the input side of the wafer. This effect indicates the presence of a weak backwards traveling wave within the wafer. Such a backward traveling wave is apparently the result of reflections at either the two grating waveguide interfaces or at the cleaned discontinuities of the waveguide ends. This effect is currently under study since it represents an undesirable optical loss channel.

FIG. 7

EXPERIMENTAL ARRANGEMENT FOR OPTICAL STUDY OF GaAs WAVEGUIDE

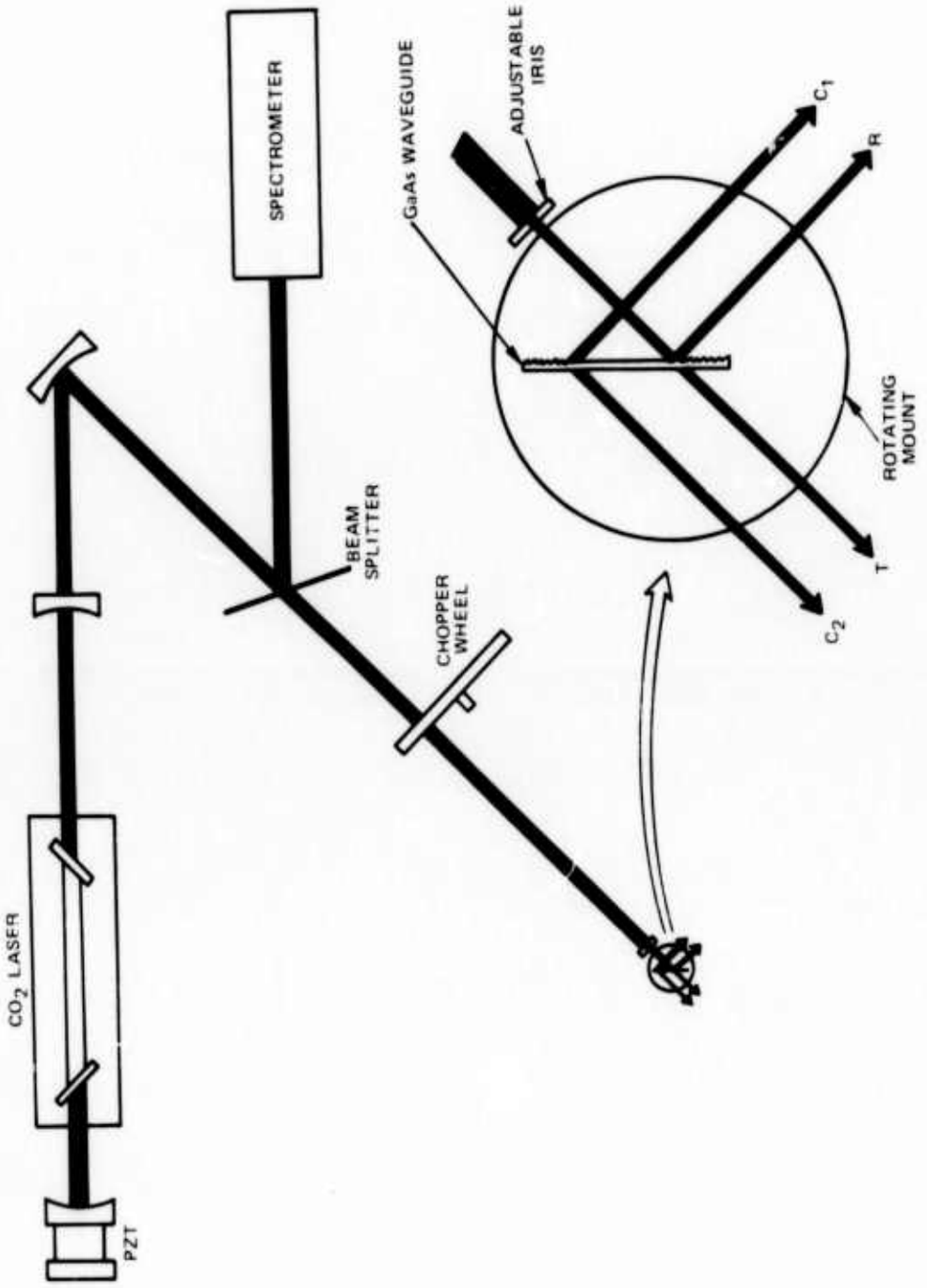

R03-181-1

After fabrication, the waveguide is mounted on a glass microscope slide that has two apertures for viewing the transmitted beam and the backcoupled beam C_2. The grating couplers are inspected under a high magnification microscope. An infrared spectrophotometer is used to test the grating structure for average thickness uniformity. Although the accuracy achievable with the spectrophotometer is limited to about 1μ thickness variation averaged over a 1 mm^2 area, this technique nonetheless provides a useful and convenient means for characterization.

During testing, the intensities in the various optical beams are monitored by an Eppley thermopile and measurements are made as a function of coupling angle and incident beam diameter. The coupled output intensity distribution is measured by moving an aperture across the outcoupled beam. The measured grating coupling angles, corresponding to a set of discrete guided-wave modes, are compared to the calculated values in Fig. 6 in order to identify the propagating modes and to determine the average waveguide thickness in the coupling region. Deviations of the coupling angles from calculated values serve as semiquantitative measures of the thickness uniformity in the coupling region. Vertical angular deviations in the coupled output beams in some cases are also observed. Such deviations can be attributed to imperfections in the waveguides and possibly result from transverse wedges perpendicular to propagation direction.

The parameter of greatest interest is the total useful coupling efficiency $\eta_{+\ell}$ (including waveguide losses). This parameter is directly determined by measuring C_1 relative to the incident beam intensity. $\eta_{+\ell}$ is sensitive to a large number of variables including incident beam diameter, guided mode number, the ratio of groove depth to average waveguide thickness in the coupling region, the groove geometry, grating separation, waveguide thickness uniformity, and the homogeneity of the coupling region as discussed in the previous section. Many of these variables are, in turn, dependent on fabrication procedures and the quality of the GaAs boules from which the waveguides are obtained.

3.4 Experimental Results and Discussion

3.4.1 Characterization of a Typical Baseline Waveguide

The baseline waveguide is a GaAs wafer, approximately 25μ thick, with two phase gratings as couplers. Neglecting waveguide propagation losses, this symmetric structure has a maximum theoretical total coupling efficiency of about 20 percent.

Parametric studies were carried out during this reporting period with detailed investigation over a dozen baseline waveguides. Parameters that were varied included waveguide thickness (22 to 28μ), thickness uniformity, grating groove depth (0.8 to 2.5μ) groove aspect ratio (0.3 to 1) and grating separation (1 to 2 cm). The groove periodicity was fixed at 2.75μ so that only backward coupling is allowed [see Eq. (1) of Ref. 5], and the grating area was fixed at 3 mm x 3 mm. Measured optical coupling efficiencies varied from < 0.5 percent to nearly 7 percent under conditions of aperture matching.

Table 3.2 summarizes the performance of a typical waveguide that provides useful coupling efficiency. This same waveguide was later coated with a thin film of gold and retested as described in Section 3.4.4. The set of coupling angles, which were determined to a precision of about 0.5 deg, were used to infer the effective thickness of the coupler region by comparing the measured coupling angles to those calculated in Fig. 6. By monitoring the energy carried by the reflected and transmitted beams at the input coupler at conditions when the incidence angle was set for maximum coupling and when the synchronous angle was misaligned by 1 deg so that the coupling reduced to zero, the amount of optical energy coupled into the waveguide could be inferred. This measurement establishes the grating input coupling efficiency for the TE_2 mode. The measured total coupling efficiency is the percent of incident light that was coupled into a single output beam (in this case C_1) and therefore includes waveguide propagation losses from scattering and absorption. Since, as apparent from Eq. (6) (cf, Fig. 10 of Ref. 5), the coupling efficiency depends on the incident beam diameter, the diameter of the adjustable aperture in Fig. 7 (and hence the incident beam diameter) was varied until maximum coupling efficiency was obtained. The beam diameters in Table 3.2 were measured along the gratings and are thus larger than the aperture diameters. Several of these measurements were repeated with the input and output couplers reversed so that the original output coupler was used at the input.

For most waveguides tested, the power P_1 in the "front" beam C_1 was approximately equal to the power P_2 in the "back" beam C_2, and the coupling efficiency was independent of whether the input laser beam was incident from the front or from the back of the waveguide. Occasionally, however, $P_1 \neq P_2$ and the coupling efficiency was different for front and back coupling. It can be shown from a reciprocity argument that the ratio of front to back coupling efficiencies should be equal to P_1/P_2. The prediction was experimentally verified. Sample #B-8, in fact, exhibited this coupling asymmetry. Care was taken with Sample #B-8 to couple through the side of the waveguide that produced the greater coupling efficiency, in this case the front (grating) side of the wafer. Analysis is currently being conducted to provide a theoretical explanation for this coupling asymmetry.

TABLE 3.2

PERFORMANCE OF A TYPICAL BASELINE WAVEGUIDE - SAMPLE #B-8

Grating Separation, cm	1.3
Groove Depth, μ	1.0
Groove Aspect Ratio	1.0
Average Waveguide Thickness, μ (Spectrophotometer)	23.0

COUPLING ANGLE-DEG*	MODE	η_{in} - %	$\eta^*_{+\ell}$ - %	OPTIMUM BEAM DIAMETER-mm	COUPLER THICKNESS-μ*
36.5 (36.5)	TE_0	†	0.3	≥ 3.0	24 ($22\frac{1}{4}$)
37.8 (38.8)	TE_1	†	2.4 (3.0)	2.5	
40.2 (41.5)	TE_2	12	4.6 (6.5)	2.0-2.5	
43.8 (46.3)	TE_3	†	4.3	1.4-2.1	
48.8 (52.8)	TE_4	†	2.1	≤ 1.5	

* Values in parentheses were obtained when the grating previously used for output coupling was used at the input. The coupler thickness was inferred from the coupling angles using the calculations in Fig. 6.

† Not measured.

3.4.2 Effects of Waveguide Thickness Variations

On the basis of the data in Table 3.2, several important observations and conclusions can be drawn. First, the waveguide thickness variation was at least 2μ over a distance of about 1.5 cm for an average taper of about 1.3μ/cm. From the analysis in Section 3.2, it appears that a thickness taper of this magnitude is not a factor in coupling efficiency. Locally, the thickness taper may have been much larger than 1.3μ/cm, however, In fact, data discussed below suggest that over small regions the effective waveguide thickness may vary by about 10μ/cm, a value that is large enough to affect the measured coupling efficiency. Effective waveguide thickness in the coupling region is defined as a combination of the local geometric thickness and the depth of the groove. The data in Table 3.2 thus should be interpreted as an indication that the variation in waveguide thickness typically achieved with present thinning techniques is of the order of 1μ. No information on the maximum taper in the coupling region is directly provided by this data.

The total coupling efficiency is less than the input efficiency because of waveguide propagation loss from scattering and absorption, the presence of two output beams as illustrated in Fig. 5, and an effective loss from light that is uncoupled by the grating. For waveguide #B-8 in Table 3.2, the amount of energy coupled into the back output beam, C_2, was aonly a small fraction of the energy in C_1. Typically, the energy in C_1 and C_2 are approximately equal. Later inspection of the wafer revealed that the back surface of the wafer lacked a high-quality specular finish. The low value of C_2 may have resulted from the poor surface condition of the back surface.

The total coupling efficiency $\eta_{+\ell}$ varied with mode number. For the lowest order modes the output grating may not have been sufficiently long to efficiently couple out all the guided light, and for the two higher order modes the effects of thickness variations, groove depth variations, or strains in the coupling region may have been especially deleterious as discussed in Section 3.2. In addition, the waveguide propagation losses for the higher order modes are greater than for the low-order modes. Since waveguide propagation losses are included in $\eta_{+\ell}$, this latter effect may account for the decreased coupling efficiency of TE_3 and TE_4. Although the general trend showing an increasing $\eta_{+\ell}$ with increasing mode number is not quantitatively understood at the present time, it is a repeatable trend that is related to the known variation of α with mode number (Ref. 5).

The higher coupling efficiencies observed when the two couplers were reversed suggests that the quality of the coupling region is an important factor in determing coupling efficiency. Since the input laser beam quality and the waveguide propagation losses were held constant for this measurement, it appears that the two couplers were not identical even though the gratings

3.4.2 Effects of Waveguide Thickness Variations

On the basis of the data in Table 3.2, several important observations and conclusions can be drawn. First, the waveguide thickness variation was at least 2μ over a distance of about 1.5 cm for an average taper of about 1.3μ/cm. From the analysis in Section 3.2, it appears that a thickness taper of this magnitude is not a factor in coupling efficiency. Locally, the thickness taper may have been much larger than 1.3μ/cm, however, In fact, data discussed below suggest that over small regions the effective waveguide thickness may vary by about 10μ/cm, a value that is large enough to affect the measured coupling efficiency. Effective waveguide thickness in the coupling region is defined as a combination of the local geometric thickness and the depth of the groove. The data in Table 3.2 thus should be interpreted as an indication that the variation in waveguide thickness typically achieved with present thinning techniques is of the order of 1μ. No information on the maximum taper in the coupling region is directly provided by this data.

The total coupling efficiency is less than the input efficiency because of waveguide propagation loss from scattering and absorption, the presence of two output beams as illustrated in Fig. 5, and an effective loss from light that is uncoupled by the grating. For waveguide #B-8 in Table 3.2, the amount of energy coupled into the back output beam, C_2, was aonly a small fraction of the energy in C_1. Typically, the energy in C_1 and C_2 are approximately equal. Later inspection of the wafer revealed that the back surface of the wafer lacked a high-quality specular finish. The low value of C_2 may have resulted from the poor surface condition of the back surface.

The total coupling efficiency $\eta_{+\ell}$ varied with mode number. For the lowest order modes the output grating may not have been sufficiently long to efficiently couple out all the guided light, and for the two higher order modes the effects of thickness variations, groove depth variations, or strains in the coupling region may have been especially deleterious as discussed in Section 3.2. In addition, the waveguide propagation losses for the higher order modes are greater than for the low-order modes. Since waveguide propagation losses are included in $\eta_{+\ell}$, this latter effect may account for the decreased coupling efficiency of TE_3 and TE_4. Although the general trend showing an increasing $\eta_{+\ell}$ with increasing mode number is not quantitatively understood at the present time, it is a repeatable trend that is related to the known variation of α with mode number (Ref. 5).

The higher coupling efficiencies observed when the two couplers were reversed suggests that the quality of the coupling region is an important factor in determing coupling efficiency. Since the input laser beam quality and the waveguide propagation losses were held constant for this measurement, it appears that the two couplers were not identical even though the gratings

had identical geometries and were fabricated under identical conditions. Measured data suggest that the average wafer thickness in the coupling region could differ by as much as 2μ. Nonreciprocity in coupling efficiency observed when the two gratings are reversed is typical even when the average thicknesses of the two coupling regions appear to be equal.

Occasionally we observe a beam steering effect which may be caused by a waveguide thickness nonuniformity transverse to the guided beam propagation direction. In the absence of a transverse taper, the input laser beam is incident in the horizontal direction (y = 0 plane), travels through the waveguide horizontally, and exits the waveguide in the same horizontal plane. The grating angle varies within this horizontal plane. If the waveguide is wedged in the y-direction, however, the beam will be steered in the y-direction within waveguide because of a prism effect and will leave the waveguide at an angle relative to the horizontal plane. For one waveguide having a grating separation of 2 cm, we have observed a beam steering angle of about 12 deg for the TE_3 mode. This particular case, which was larger than typical, has been analyzed by a simple calculation as given below. It is important to note that the coupling efficiencies obtained with this latter waveguide structure were comparable to those obtained with sample #B-8 even though the beam steering for #B-8 was only about 2 deg. The beam steering does not appear to be a sensitive indication of the quality of the coupling region, therefore. It is considered here only because the beam steering provides another indication of the magnitude of thickness variations that can exist in the present waveguide structures.

If the waveguide has a transverse wedge, the value of β/k will change in the transverse (y) direction as apparent from the calculation in Fig. 6 and from the discussion on pp. 14 of Ref. 5. As a consequence, the phase velocity of the wave will change with y. One side of the beam will move faster than the other side and the phase front will bend in the direction of slower portion (Ref. 6). If n denotes the effective index of refraction of the waveguide defined as the ratio of the vacuum speed of light to the phase velocity in the guide, then two light rays A and B on opposite sides of the guided mode (see Fig. 8) will travel a different optical distance with the difference equal to $L\,\Delta n/\ell$, where L is the propagation length assumed to be equal to the separation of the two grating couplers and ℓ is the beam width in the y-direction. The beam will then be deflected in the y-direction by an angle.

$$\theta_G \cong \frac{L\Delta n}{\ell} . \tag{13}$$

When the beam leaves the waveguide, the deflection angle will be further increased according to Snell's law. Since the index of refraction of GaAs is about 3.3, the deflection angle will be increased to about

FIG. 8

BEAM DEFLECTION INDUCED BY TRANSVERSE CHANGE IN PHASE VELOCITY

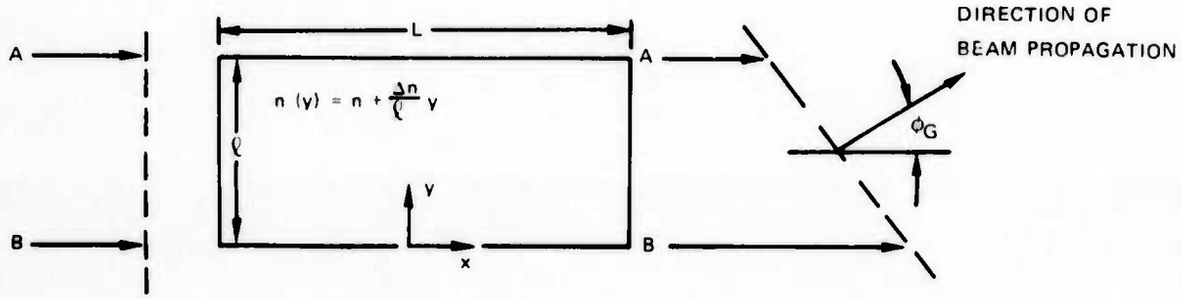

R03-182-1

$$\phi \cong 3.3 \frac{L\Delta n}{\ell} . \tag{14}$$

The value of Δn can be related to a change in waveguide thickness. Using standard waveguide analysis, it can be shown that the fraction change $\Delta n/n$ is approximately related to the fractional thickness change $\Delta t/t$ by

$$\frac{\Delta n}{n} \cong 0.063 \frac{\Delta t}{t} \tag{15}$$

for the TE_3 mode and an average waveguide thickness of 25μ.

Equations (14) and (15) can be used to calculate the magnitude of the transverse taper necessary to steer the beam by 12 deg = 0.21 rad. Defining the taper as $\Delta t/\ell$, we find

$$\frac{\Delta t}{\ell} = 4.8 \frac{t}{nL} \phi \tag{16}$$

Letting t = 25μ, L = 2 cm and n = 3.1 (where $n < n_{GaAs}$ for all guided modes),

$$\frac{\Delta t}{\ell} = 4.1 \times 10^{-4} = 0.41 \ \mu/\text{mm}. \tag{17}$$

The magnitude of $\Delta t/\ell$ is of the correct magnitude to significantly affect the coupling efficiency. The beam steering data which is largely determined by propagation in the waveguide between the couplers, thus provides another indication that thickness variations in presently available waveguides are large enough to be a factor in the optical coupling characteristics of the structures.

3.4.3 Effects of Grating Groove Depth

The data obtained in Table 3.2 was obtained under aperture-match or near aperture-matched conditions. For the actual thin-film modulator, the width of the mini-gap ridge restricts the maximum beam width in the y-direction to < 1 mm. If a circular beam is used at the input, then the input beam diameter ℓ (relative to the waveguide plane) that will be used in practice is < 1 mm/cos θ_G where θ_G is the input coupling angle. For TE_1, cos $\theta_G \cong 38$ deg so that $\ell < 1.27$ mm. In order to test the coupling efficiency for a small-diameter input beam, measurements with the most recent samples having very deep grooves ($\delta \approx 2.5\mu$) have been obtained with a tightly focused beam having a beam waist of 0.75 mm so that $\ell = 0.75/\cos \theta_G$. Table 3.3 summarizes a partial list of data showing that reasonable coupling efficiency can be obtained for low-order modes with a sufficiently small input beam diameter. This waveguide structure is the same type of structure that will be used for the next phase of thin-film modulator experiments. Either the TE_1 or the TE_2 mode will be used in these experiments.

TABLE 3.3

PERFORMANCE OF BASELINE WAVEGUIDE - SAMPLE #B-9

Grating Separation, cm	2.0
Groove Depth, μ	2.5
Groove Aspect Ratio	1.0
Average Waveguide Thickness, μ (Spectrophotometer)	27.0
Input Beam Diameter, mm	$0.75/\sin \theta_G$

Coupling Angle θ_G - deg	Mode	$T_{4\ell}$ - %
36.6	TE_0	0.6
38.0	TE_1	2.1
39.9	TE_2	4.6

3.4.4 Intensity Distribution of Outcoupled Beams

The intensity distribution of the outcoupled beams have been measured by moving either a blocking aperture or a slit aperture across the output grating and measuring the energy transmitted past the aperture as a function of the aperture position. These measurements were conducted because they provide a sensitive indication of the quality of the output coupling grating.

As discussed in Section 3.2, the near-field of the coupled output beam for a uniform grating has the form of the characteristic aperture function;

$$I(x) \propto [E(x)]^2 \propto \exp(-2\alpha x) \tag{18}$$

where x is measured along the grating in the direction of propagation and $x = 0$ at the inside edge of the output grating. If a blocking aperture is placed on the grating and then moved in the $\pm x$ direction so as to expose a progressively larger portion of the grating, then the optical energy w coupled out will have the form

$$w(x) = w_o [1 - \exp(-2\alpha x)] \tag{19}$$

where w_o is a constant and Eq. (5) has been used. If α varies with position because of thikness variations or strains in the coupling region or because of grating variations, then I(x) will not have a simple exponential shape.

Figure 9 shows the results of a scan conducted with an early waveguide structure. I(x) was inferred by fitting the measured values of w(x) to Eq. (19). The grating used had a small value of α so that only a high-order mode such as TE_5 could be excited. This data represents the closest match yet obtained between the inferred output intensity distribution and Eq. (18). Because the data reproduced the exponential curve so closely, a value of α could be obtained and compared to a theoretical value that was calculated using approximate scaling laws. These scaling laws will be discussed in the next reporting period.

In general, the output beam intensity distribution does not have the smooth form of the data in Fig. 9. Structure in I(x) and deviation from the exponential shape suggests that the coupler is not homogeneous. Output intensity scans are being conducted on each sample and will hopefully provide useful information on the quality of the waveguide structures.

FIG. 9

INTENSITY DISTRIBUTION OF OUTCOUPLED BEAM

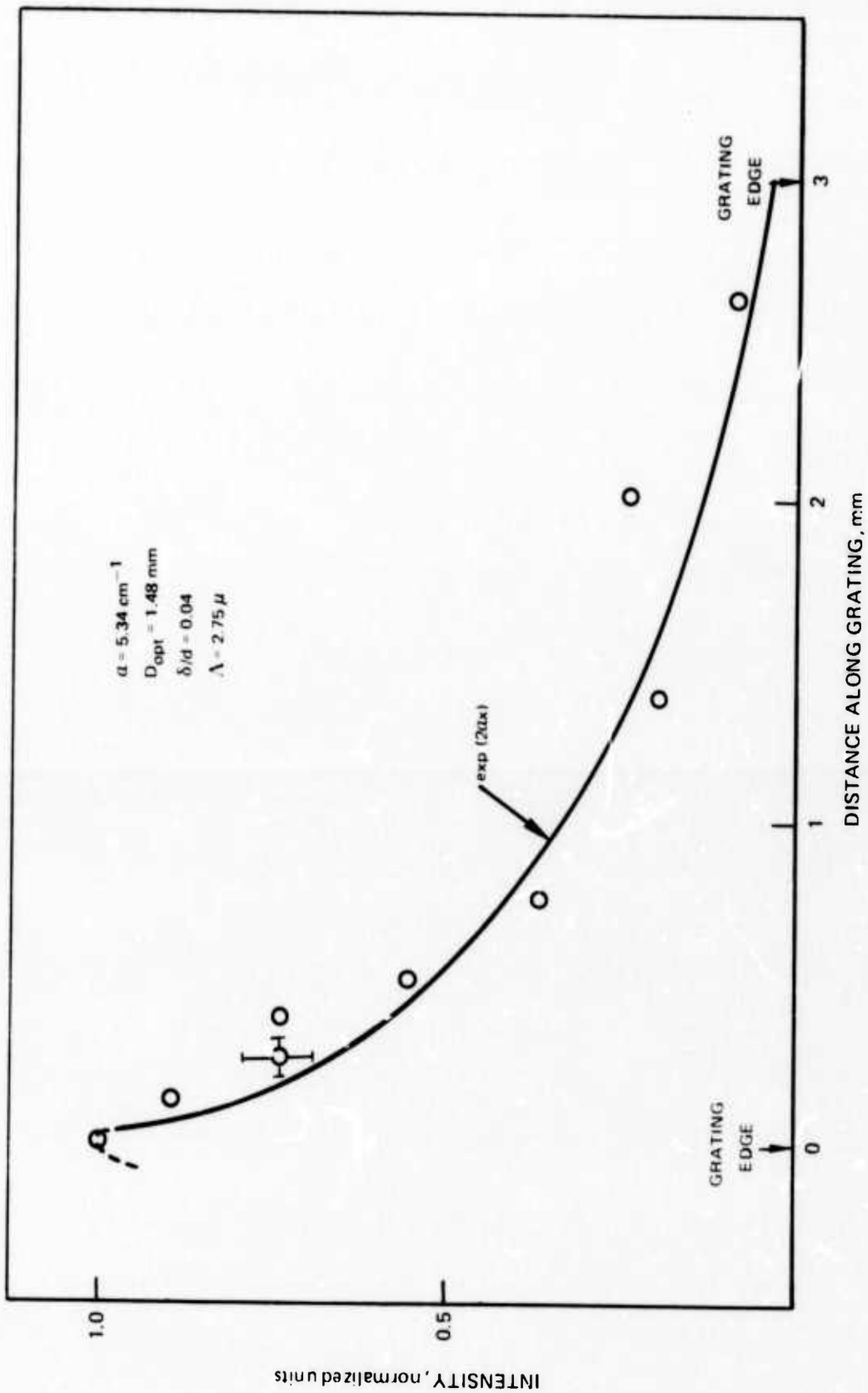

R03-159-1

3.4.5 Metallized Waveguide With Grating Couplers

It was suggested in the previous technical report that metallizing one side of the waveguide will increase the total effective coupling efficiency. An increase was expected because the transmitted beam and the back outcoupled beam (C_2 in Fig. 5) would be reflected at the metal-waveguide interface. The energy contained in those unwanted beams should be at least partially redirected into the guided beam and the useful output beam C_1, respectively. In addition, it was noted that the metal film would both reduce microwave losses in the modulator by eliminating air gaps and reduce wafer breakage that resulted from the necessity to force the mini-gap ridge onto the GaAs wafer.

During this reporting period, the effects of a thin gold film vacuum-deposited on the back of a GaAs waveguide structure were investigated with a limited set of measurements. As apparent from the data in Table 3.4, the metal coating did not produce the desired effect on optical coupling efficiency. In fact, because of the increase in waveguide propagation losses due to absorption in the metal layer, the total coupling efficiency which includes propagation losses actually decreased.

The optical loss caused by a gold layer as a function of waveguide thickness and mode number has been calculated for a GaAs waveguide (Ref. 7). According to those calculations, over a 1.5 propagation path (which includes the relevant portions of the two coupling regions) about 1/3 of the energy in TE_2 should be lost to absorption whereas experimentally nearly 2/3 of the guided energy appeared to be lost to absorption in the gold film. The increased loss is apparently due to the imperfect nature of the metal-GaAs interface. As noted in Section 3.4.1, the back of sample #B-8 which was coated for these measurements did not have a high quality specular finish. A more carefully polished waveguide may have lower attenuation, in closer agreement with theory.

The propagation losses are expected to decrease rapidly with decreasing mode number, because the effective number of bounces per unit distance experienced by a guided mode decreases for the low-order modes (Ref. 7). Experimentally, it was found that the TE_1 mode appeared to lose only about 1/3 of its energy, decreasing from 3.0 percent (see Table 3.2) to 2.1 percent. This value is also about a factor of two larger than predicted by theory.

Despite the loss in total coupling efficiency created by the metal film, such a film may yet be useful for the final modulator configuration because of the microwave and handling advantages inherent in its use. Further work will attempt to decrease the losses introduced by the film. The effects of both a specular finish at the gold-GaAs interface and improved gold vacuum deposition techniques will be investigated, and the use of a thin buffer layer of ZnSe or other suitable material will be considered.

TABLE 3.4

EFFECTS OF METAL LAYER ON COUPLING

CHARACTERISTICS OF TE_2 - SAMPLE #B-8

INPUT GRATING	WAVEGUIDE	COUPLING ANGLE-DEG	η_{in} - %	$\tau_{+\ell}$ - %
1	No Metal	40.2 ± 0.3	12 ± 2	4.6 ± 0.5
	With Metal	40.3 ± 0.3	15 ± 3	1.7 ± 0.2
2	No Metal	39.9 ± 0.3	*	6.5 ± 0.7
	With Metal	41.4 ± 0.3	24 ± 4	2.2 ± 0.2

* Not Measured.

3.4.6 Prism Coupling

The use of a prism coupler should, in principle, increase both the input and output coupling efficiencies by about a factor of 2. This predicted improvement results from the elimination of the transmitted beam at the input and the unwanted back output beam C_2 (see Fig. 5). In early work it was found that the use of a prism coupler created large stresses in the thin waveguides, causing them to fracture. Improved fabrication and bonding techniques have considerably reduced this difficulty. In fact, techniques have been advanced to the point where prism couplers can now be considered for use in the thin-film modulator.

In order to assess the attractiveness of prism couplers for the modulator application, a set of preliminary experiments that used one prism coupler and one grating coupler were conducted. This particular "hybrid" coupler configuration, which was selected for experimental convenience, may be attractive for the actual thin-film modulator.

Coupling through a prism occurs through the process of frustrated total internal reflection (Ref. 8). The mathematical description of the coupling process is formally the same as the description of coupling through a grating with the exceptions that the coupling angles and the attenuation coefficient α are, of course, given by different relationships.

The input coupling angles ϕ for the prism are functions of β/k of the propagating mode and the relevant indices of refraction. It is convenient to relate ϕ to the grating coupling angle θ_G for the "hybrid" coupler by using Fig. 10. The relationship connecting ϕ and θ_G, assuming that the thicknesses of the two coupling regions are equal, is given by

$$\phi = \frac{\pi}{4} + \arcsin \left\{ n_3 \sin \left| \arcsin \left(\frac{1}{n_3} \left(\frac{\lambda}{\Lambda} - \sin \theta_G \right) \right) - \frac{\pi}{4} \right| \right\} \qquad (20)$$

where n_1, n_2, n_3 are the indices of refraction of the Ge coupling prism, the gap under the prism, and the GaAs waveguide, respectively. As before, the grating groove periodicity Λ is taken as 2.75μ and a wavelength λ = 10.6μ is used.

The attenuation coefficient α is related to appropriate waveguide and coupler parameters by Eq. (17) of Ref. 8. Its value depends on the gap size, the three indices of refraction, the waveguide thickness in the coupling region, and the mode number. Equation (5) in Section 3.2 can be used to determine the coupling efficiency if the factor of $\frac{1}{2}$ is dropped from the relationship. For a uniform coupling region and no coupling angle error, η is given

FIG. 10

RELATIONSHIP BETWEEN GRATING AND PRISM COUPLING ANGLES

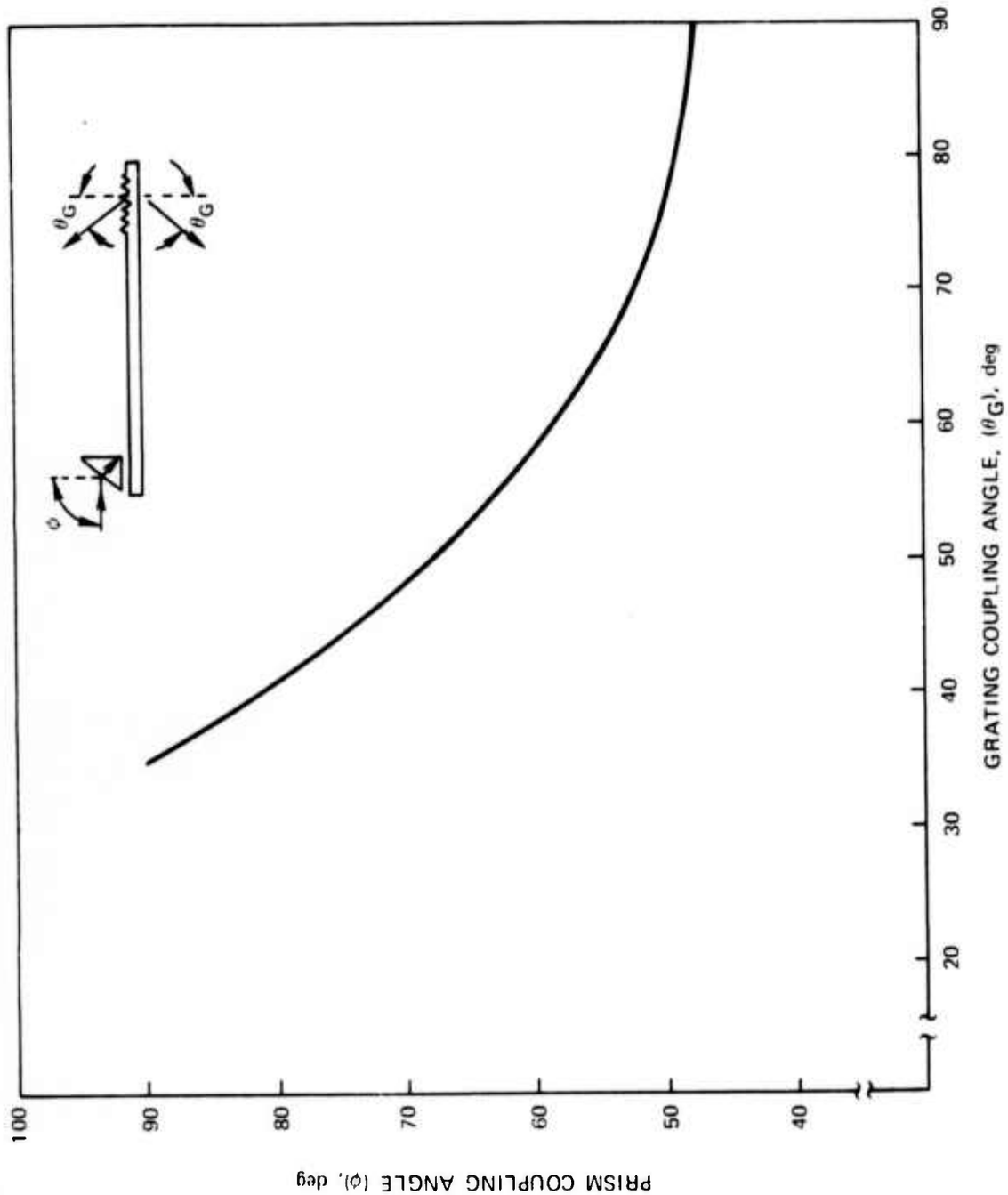

R03-151-2

by F in Eq. (6). Using these theoretical relationships, we have calculated η as a function of gap size, n_2 and θ_G for $n_1 = 4.0$(Ge), $n_2 = 3.275$(GaAs), and an input beam diameter $\ell = 1$ mm. As before, θ_G was chosen as parameter for the calculation instead of β/k which appears explicitly in the theory because θ_G is a directly measurable parameter that is simply related to β/k by the grating equation.

The calculated maximum values of η are shown in Fig. 11. In practice, η is degraded by thickness variations in the coupling region, gap variations, etc. It is seen from Fig. 11 that the optimum gap size d_{opt} increases with increasing θ_G (or, equivalently, with decreasing β/k or increasing mode number). The value of d_{opt} also increases with increasing n_2 because increasing n_2 tends to extend the evanescent tail of the guided mode. When an air gap is used, d_{opt} is about 0.25μ for the TE_1 mode and about 0.3μ for TE_2.

A "hybrid" coupler was configured using a waveguide with a single grating. A Ge prism coupler, positioned about 2 cm from the grating, was placed on the waveguide. Although the air gap between the prism and the waveguide was not externally controlled, a gap of about 0.3μ was naturally achieved by simply removing the largest dust particles from the GaAs wafer prior to positioning of the prism. The set of grating input coupling angles θ_G were measured first with the prism used as an output coupler. Reversing the roles of the couplers, the prism coupling angles ϕ were accurately measured and the corresponding values of θ_G and ϕ were compared to the calculations in Fig. 10. The agreement was within a fraction of a degree, thus indicating that the average thickness of the coupling regions were nearly identical. The coupling efficiencies were measured for both arrangements with a 0.75 mm input beam.

With the grating used as the input coupler, the total transmission coefficient for TE_1 was nearly 5 percent. This value compares to a best value for TE_1 of about 3 percent for a baseline waveguide with two gratings. When the prism was used as the input coupler, the useful coupling efficiency appeared to increase, but the measurements were confused by the back coupled beam that was reflected off a glass mount on which the waveguide was positioned. In principle, if the uniformity of the two coupling regions are nearly the same, and the input beam is properly adjusted in size so that aperture-matching is achieved, the useful coupling efficiency will be the same whether the prism is used as the input coupler or the output coupler.

These preliminary measurements are extremely encouraging. They demonstrated that prism couplers can be used without waveguide failure and suggest that the total optical coupling efficiency can be significantly increased for the low-order modes of interest in the modulator device. Additional study will be conducted during the next reporting period to determine if the high coupling efficiency observed with this waveguide structure is repeatable. Techniques for controlling the prism-waveguide gap and simplifying the prism mounting procedure will be investigated.

INPUT COUPLING EFFICIENCY FOR PRISM COUPLER WITH INPUT BEAM DIAMETER OF 1 mm

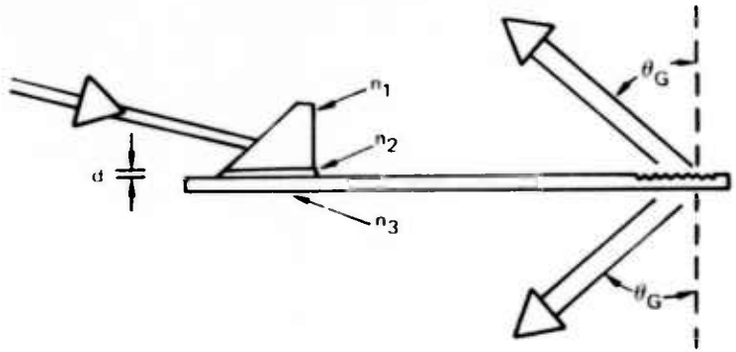

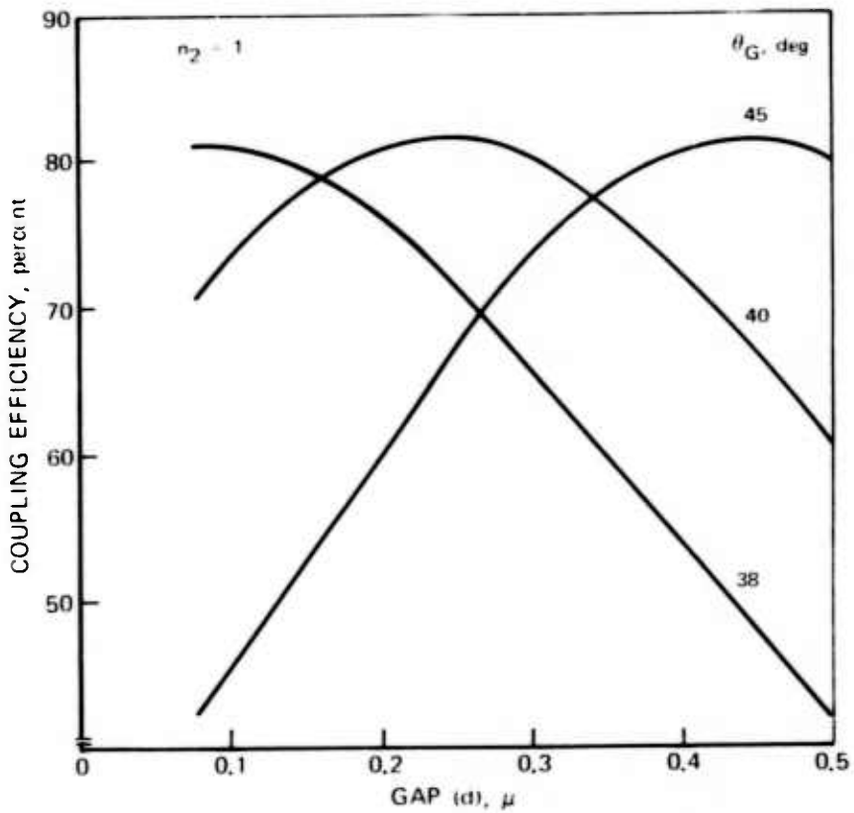

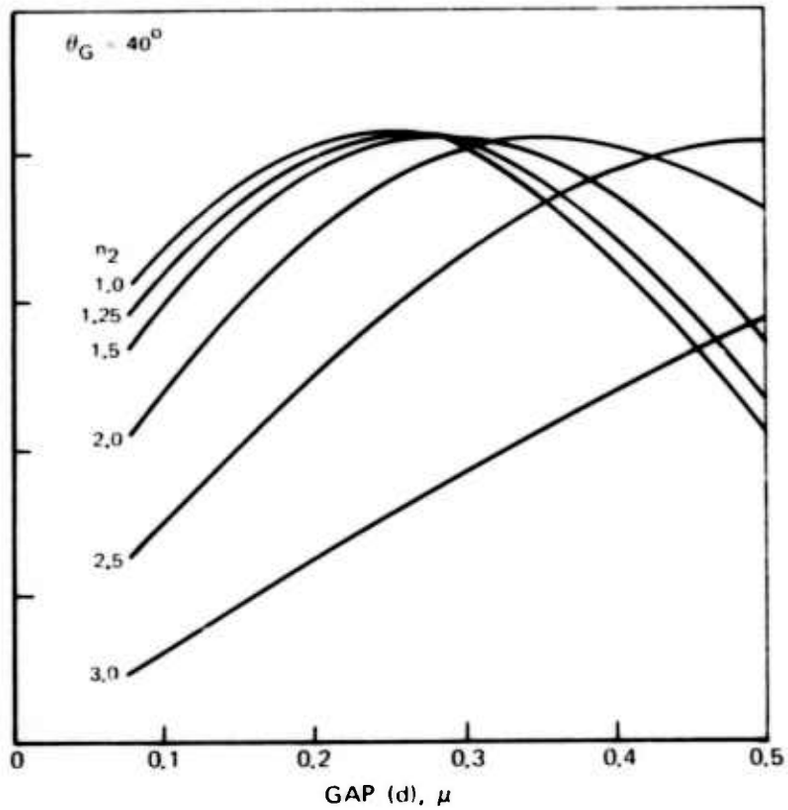

FIG. 11

R03-144-2

3.4.7 Optical Damage

The development of a practical thin-film modulator requires that the waveguide be capable of withstanding input laser powers of about 20 W focused into a 1 mm diameter beam without optical damage. Under these conditions, the average laser intensity across the beam is 2.5 kW/cm^2. If the beam is gaussian with a beam diameter ($1/e^2$ in intensity) of 1 mm, the peak intensity of the beam on axis will be 5 kW/cm^2. A laser intensity of 5 kW/cm^2 is well below intrinsic damage limits.

To test the damage susceptibility of both the GaAs waveguide and a waveguide with a Au film vacuum deposited on the back surface, a gaussian laser beam with a power of about 2.33 W was focused to a diameter of 0.4 mm and the waveguide grating couplers were placed at the focus in turn. The resulting intensity on axis was 3.7 kW/cm^2. No damage was observed with either waveguide. Because the experiment did not induce optical damage and increased laser power was not available at the time, it was not possible to establish damage limits.

This experiment does demonstrate, however, that incident intensities of up to 15 W in 1 mm focused laser beams will not damage either the baseline structure of the metal-back waveguide. During the next reporting period, these waveguides will be tested with laser intensities in excess of 5 kW/cm^2.

3.4.8 Summary

In summary, the maximum useful coupling efficiency obtained with present structures is nearly 7 percent which is sufficient to obtain 25 mW of sideband power under the conditions of Fig. 1. A total optical transmission of 7 percent is within a factor of 3 of theoretical maximum. Experimental data suggests that imperfections in the waveguide region account for part of the difference between theory and experiment. Although reproduceable data has not yet been obtained on waveguide propagation losses, it appears that such losses may account for the rest of this difference. No significant mode conversion was observed in any of the more recently fabricated waveguides.

3.5 Conclusions

In this section, analysis and experimental data describing the optical coupling characteristics of three types of waveguide structures have been presented. These structures are a symmetric GaAs wafer with etched phase grating couplers, a metal-coated wafer with grating couplers, and a symmetric wafer with one prism and one grating coupler. It has been shown that waveguide imperfections, particularly localized thickness variations in the coupling region,

appear to be important factors in optical coupling, accounting for a measurable loss in available coupled power. Such imperfections are to be expected because of the extreme technical complexity of fabricating free-standing GaAs wafers with thicknesses of only 25μ and areas in excess of 2 cm^2.

In view of the fabrication complexities, the performance achieved with these waveguides has been encouraging. Total optical coupling efficiencies into a single output beam of nearly 7 percent (including waveguide losses) have been obtained with the baseline structure and the TE_2 mode. Such efficiencies are within a factor of about 3 of maximum coupling efficiencies for an ideal lossless structure, and they are sufficiently high to permit 20 mW of sideband power generation for the conditions of Fig. 1.

Advanced fabrication techniques are currently under development. These include methods of bonding the wafer to the modulator baseplate prior to final thinning, improved grating etching procedures, and rf sputtering of ZnSe thin buffer layers on GaAs substrate. If successful, these advanced techniques may provide additional improvements in useful coupling efficiency with a corresponding increase in available sideband power. Because these techniques will also tend to enhance the wafer mechanical strength, the use of prism couplers in a practical device should become possible. Coupling with prisms is expected to increase the useful coupling efficiencies by a factor of 2 or more beyond the efficiencies available with grating couplers.

The advances achieved during the present reporting period represent an important milestone in the current program. Detailed evaluation of optical waveguides has provided useful information which is needed for the development of a practical thin-film modulator. During the next reporting period, the coupling studies and the development of fabrication techniques will be continued, and a series of microwave modulator experiments will be conducted.

The development of a prototype thin-film modulator appears feasible in the near term. Such a device will be the first practical device to evolve from integrated optics technology. Its development will provide an important contribution to the needs of optical radar and middle-infrared laser systems.

4.0 REFERENCES

1. P. K. Cheo, M. Gilden, D. W. Fradin and R. Wagner, "Microwave Waveguide Modulators for CO_2 Lasers", Fourth UARL Semi-Annual Technical Report N921513-8, Contract No. N00014-73-C-0087 (September 1974).

2. S. T. Peng and T. Tamir, Opt. Communications (to be published).

3. A. D. Pearson, et. al., "Chemical Physics, and Electrical Properties of Some Unusual Inorganic Glasses", 6th International Congress on Glass, Vol. I, Advances in Glass Technology, 357 (1962).

4. W. R. Northover, "Chalcogenide Glass as a Bonding Agent for Ultrasonic Delay Lines", Proc. International Comm. on Glass, 113 (1969).

5. P. K. Cheo, M. Gilden, D. W. Fradin and R. Wagner, "Microwave Waveguide Modulators for CO_2 Lasers", Third UARL Semi-Annual Report N921513-6, Contract No. N00014-73-C-0087 (March 1974).

6. A. Yariv, Introduction to Optical Electronics: (Holt, Rhinhardt and Winston, 1971), p. 243.

7. P. K. Cheo, J. M. Berak, W. Oshinsky and J. L. Swindal, "Optical Waveguide Structures for CO_2 Lasers", Appl. Opt. 12, 500 (1973); see Fig. 4 and Appendix 3.

8. P. K. Tien, "Light Waves in Thin Films and Integrated Optics", Appl. Opt. 10, 2395 (1971).